JCTC Journal of Chemical Theory and Computation

Analysis of the Primary Photocycle Reactions Occurring in the Light, Oxygen, and Voltage Blue-Light Receptor by Multiconfigurational Quantum-Chemical Methods

Tatiana Domratcheva,* Roman Fedorov,† and Ilme Schlichting

Max-Planck Institute for Medical Research, Department of Biomolecular Mechanisms, Jahnstrasse 29, 69120 Heidelberg, Germany

Received January 8, 2006

Abstract: The photocycle reactions occurring between the flavin mononucleotide cofactor and the reactive cysteine residue in the blue-light photoreceptor domain light, oxygen, and voltage (LOV) were modeled for a system consisting of lumiflavin and thiomethanol. The electronic structure and energies of the reactive species were estimated using the CASSCF and MCQDPT2 quantum-chemical methods. The reaction pathway for the S−C4a covalent adduct formation in the triplet state was determined. Concerted electron and proton transfer from the thiol to the flavin in the triplet electronic state results in a biradical complex that is, however, unstable because its structure corresponds to a triplet−singlet crossing. The covalent adduct dissociation in the ground electronic state is a reverse of the photoreaction proceeding via a single energy barrier for hydrogen transfer. Thus, both photo- and dark reactions were found to be single-step chemical transformations occurring without stable intermediates. The photoreaction yielding the S−C4a covalent adduct is an intrinsic property of the isoalloxazine−thiol complex in the specific geometry arranged by the protein in LOV. The S−C4a covalent adduct between lumiflavin and thiomethanol is rather stable implying that in LOV its dissociation is facilitated by the protein.

Introduction

To increase the efficiency of photosynthesis, plants use blue-light receptor proteins called phototropins[1] that are involved in phototropism, light-induced stomatal opening, and chloroplast movement to places with appropriate light intensity. Phototropins are light-driven autophosphorylating protein kinases that contain two similar, but not identical, light-receptor domains LOV1 and LOV2.[2−4] Each light, oxygen, and voltage (LOV) domain binds noncovalently a flavin mononucleotide (FMN) chromophore that undergoes a photoreaction upon blue-light absorption. Photoexcited FMN and a conserved cysteine (Cys) residue form a S−C4a flavin-cysteinyl covalent adduct (Scheme 1) on a microsecond scale.[5,6] In the dark, the photoproduct dissociates into the initial components within minutes. The LOV photoproduct triggers autophosphorylation of the kinase, which initiates the phototropism-signaling reaction cascade.

Light-induced changes in absorbance have been detected for the LOV domains.[7,8] Upon illumination by blue light, the FMN absorption band at 447 nm bleaches. A transient absorption band at about 700 nm of a triplet flavin species is formed within nanoseconds. Then, a broad band of the covalent adduct appears with a maximum at 390 nm. In the dark, the FMN absorption band at 447 nm recovers because of thermal dissociation of the adduct into the initial components.

Several hypotheses of the mechanism of the covalent adduct formation in LOV have been put forward. The increase of the basic properties of flavins upon photoexcitation is well-known[9−12] and expected to play a role in the LOV photochemistry.[13,14] In the triplet state, a protonated cation of FMN ($HFMN^+$) can be formed. An ionic mecha-

* Corresponding author phone: +49-6221-486-504; fax: 49 6221 486 585; e-mail: Tatjana.Domratcheva@mpimf-heidelberg-.mpg.de.

† Current address: Department of Biophysical Chemistry, OE4350 Hannover Medical School, Carl-Neuberg-Strasse 1, 30625 Hannover, Germany.

10.1021/ct0600114 CCC: $33.50
Published on Web 09/14/2006

Scheme 1

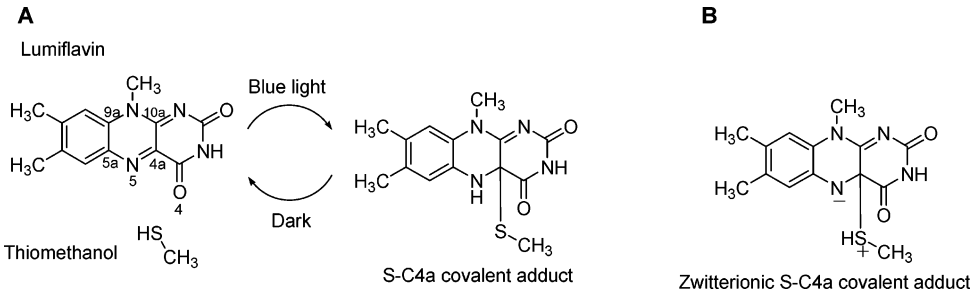

nism of the S−C4a covalent adduct formation[8,14] implies an interaction of the thiolate anion with the C4a atom of $HFMN^+$. However, there is no experimental evidence for stable or transient ionic species occurring in the LOV photocycle. FTIR spectra showed that the cysteine was protonated in the LOV dark-adopted state,[15] while electron paramagnetic resonance (EPR) measurements excluded a protonation of the triplet FMN intermediate.[16,17] Flavins are potent oxidants for redox-active amino acids such as cysteine.[18] Hence, a radical mechanism has been proposed.[16,17,19,20] An ionic radical pair was predicted to form as a result of a one-electron reduction of FMN by the cysteine. At cryogenic temperature, the radical pair recombines resulting in the S−C4a zwitterionic covalent adduct that at room temperature converts to the S−C4a covalent adduct by proton transfer. However, the FMN radicals were detected only in light-excited LOV mutants[17,19−21] but not in the wild-type LOV.[16] In our previous work, we discussed a concerted mechanism based on quantum-chemical analysis of the crystal structures of the LOV1 domain.[13] Proton transfer from the cysteine to the N5 atom of the triplet FMN is concerted with the S−C4a covalent bond formation.

After the X-ray crystal structures of both dark-adopted and light-illuminated states of the LOV domains were determined,[13,22,23] the photoreaction mechanism was addressed by means of quantum-chemical calculations.[13,24,25] The analysis of the electronic structure of the isoalloxazine chromophore in the ground singlet and excited triplet states by complete active space self-consistent field (CASSCF) calculations[13] favored a concerted mechanism. Energy estimates by density functional theory (DFT) showed that a radical pair between FMN-related molecules and a thiol is more favorable than the corresponding ion pair.[24] A stable radical pair intermediate along the photoreaction pathway was predicted by Hartree−Fock- (HF-)based quantum-mechanical/molecular-mechanical (QM/MM) modeling supporting the radical mechanism hypothesis.[25] Nevertheless, the LOV quantum-chemical analysis is far from being complete. To describe the electronic excitations, the excited-state reaction pathway, and the S−C4a covalent bond dissociation in the ground state, it is necessary to go beyond single-configurational methods such as HF and DFT. Experimental data,[26] the QM/MM model,[25] and our previous calculations[13] indicate strongly that the primary photoreaction in LOV is localized within the FMN-reactive Cys subsystem. Therefore, a model system consisting of an isoalloxazine chromophore and a thiol can be used for the high-level quantum-chemical analysis.

In the present study, we analyze the LOV photocycle reactions using a lumiflavin-thiomethanol model complex (Scheme 1A) and CASSCF calculations supplemented with second-order multiconfigurational perturbation theory (MC-QDPT2). The electronic structure of the photospecies is described, and accurate energy estimates are obtained. The derived energy profile of both photo- and dark reactions is consistent with a concerted mechanism.

Computational Details

A model system consisting of lumiflavin and thiomethanol is depicted in Scheme 1A; the atom numbering used throughout the text is indicated. Lumiflavin contains the dimethylisoalloxazine ring of FMN; thiomethanol represents the side chain of the reactive cysteine. The starting geometries were taken from the crystal structures of LOV1 from *Chlamydomonas reinhardtii*[13] (reagent and covalent adduct complex PDB codes 1n9l and 1n9o, respectively). Geometry optimization of the model complexes was carried out in the internal coordinates.[27] Restrained geometry optimization was used to ensure the arrangement of the reagents as in the LOV domain, where the side chain of the cysteine is located above the isoalloxazine ring. The optimized structures are in good agreement with the ones obtained in the QM/MM study of LOV[25] where the geometry of a quantum-chemically described lumiflavin−thiomethanol complex was restrained by the molecular-mechanical model of the LOV protein.

CASSCF[28] and MCQDPT2[29] calculations with a standard Gaussian basis set 6-31G(d) containing polarization d functions for the heavy atoms were carried out to derive the energy profile of the photocycle reactions and to evaluate the electronic and absorption properties of the model complexes. The lumiflavin−thiomethanol complex has 160 electrons, which are described by 351 single-electron wave functions—molecular orbitals (MOs)—when the 6-31G(d) basis set is used. The active space is indicated by the numbers in parentheses CASSCF(n,m), where n is the number of electrons and m is the number of MOs. The multireference configurational interaction (MRCI) method was used to validate the choice of the active space. The configuration interaction (CI) calculations accounting for single and double electronic excitations (CI−SD) were done with the molecular orbitals obtained from the CASSCF calculations (hereafter referred to as MRCI−SD calculations). A total of 65 MOs were considered to be core orbitals and 256 MOs to be virtual, yielding a MRCI−SD solution accounting for electronic excitations within a window of 30 MOs with 30 electrons sufficiently large for our purposes because it

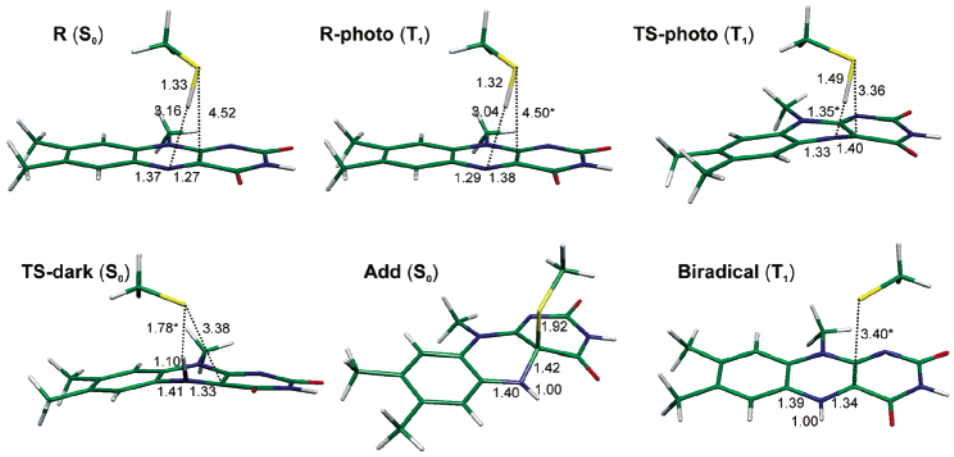

Figure 1. Structures of the model complexes optimized by the CASSCF(2,2)/6-31G(d) method. The electronic state is indicated in parentheses. Selected distances are specified in angstroms. The distances marked by an asterisk were fixed during geometry optimization.

contained all π MOs (7π and $7\pi^*$). The dynamic electron correlation not accounted for by the CASSCF(2,2) or (4,4) method was taken into consideration by single-point MC-QDPT2 calculations.

To optimize geometries, state-specific CASSCF(2,2) calculations were used. To describe the charge distribution, Löwdin[30] and Mulliken[31] atomic electrostatic charges were calculated. Both methods provided consistent results, but the Mulliken charges were somewhat overestimated. Therefore, Löwdin atomic charges are presented in the text. To evaluate the electronic transition energies of the reactive species, MCQDPT2/CASSCF calculations with the state-averaged energy functional were performed. The CASSCF equations were solved with the averaged density from the two electronic states involved in the transition with weight coefficients 0.5 and 0.5. The calculations were done using the PC GAMESS version[32] of the GAMESS (U.S.) quantum-chemical program package.[33] The program Molekel[34] was used to create the figures.

We extensively compare our results on the "free complex" (i.e., not embedded in the protein) with the QM/MM calculations[25] to analyze the effect of the protein matrix, which is not included in our model, as well as the effects of electron correlation, which are not accounted for in the QM/MM model.

Results and Discussion

In the photoreaction, the excited triplet flavin interacts with the cysteine to form the S−C4a-covalent adduct (Scheme 1A). In the dark-reaction, occurring in the ground electronic state, the photoproduct dissociates. To obtain the energy profile of the photocycle, the following structures were optimized by the CASSCF(2,2) method: (1) the lumiflavin−thiomethanol complex **R** optimized in the ground state (dark-adapted state of LOV absorbing at 447 nm), (2) the lumiflavin−thiomethanol complex **R-photo** optimized in the triplet state (the spectroscopically characterized triplet intermediate absorbing at 660 and 715 nm), (3) the highest-energy structure for the H-transfer reaction between S−H and N5 in the triplet state **TS-photo**—a model for the photoreaction transition state, (4) the triplet **Biradical** complex between two radicals SCH_3 and N5H-semiquinone, which is a product of the H-transfer reaction, (5) the S−C4a covalent adduct **Add** optimized in the ground state (the photoproduct state of LOV absorbing at 390 nm), and (6) the structure **TS-dark** in the ground state similar to **TS-photo** and representing a transition state for the **Add** conversion into the initial complex **R**. All structures are presented in Figure 1.

The calculated energies and CI coefficients of the wave functions obtained by different multiconfigurational methods are presented in Table 1. The state-specific CASSCF(2,2) solutions were obtained with the active space containing the highest occupied and lowest uncoupled molecular orbitals (HOMO and LUMO) of the ground-state Hartree−Fock electronic configuration. For complexes **R** in S_0 and S_1 and **Add** in S_0, the CASSCF(2,2) wave functions mainly consist of a single determinant. For geometries **Biradical** and **TS-dark** in the S_0 state, a two-configurational wave function is required to account for the dissociated S−C4a covalent bond. The CASSCF(2,2) solutions for the triplet state are identical to the ROHF solutions. To determine if the active space needs to be extended, the MRCI−SD calculations with CASSCF(2,2) MOs were performed. The MRCI−SD energies are lower, compared to the CASSCF(2,2) energies, but the CI coefficients obtained by the two methods are in agreement. Only minor contributing configuration state functions (CSFs) whose MRCI coefficients do not exceed 0.1 (the largest value, 0.12, was obtained for the S_1 solution at the **R** geometry) corresponding to the excitations outside the (2,2) active space were found. These excitations occur within a pair of the π,π^* MOs localized on the dimethylbenzene ring. The orbitals were included into the active space to obtain CASSCF(4,4) solutions. For the **Add** geometry in S_0, only double excitations from HOMO to LUMO were found to be significant. Accordingly, the energies of **Add** calculated by the CASSCF(2,2) and MRCI−SD methods differ only by 0.3 kcal/mol. Our attempts to obtain the CASSCF(4,4) solution for **Add** that would be similar to the solutions obtained for the other model complexes were unsuccessful because the CASSCF iterations did not converge. For the other model complexes, the extension of the

Table 1. Total Energies (Hartree) and Compositions of the Wave Functions Given by the CI Coefficients of the Dominant Configuration State Functions (CSFs)

structure[a]	**R**	**R**	**R**	**R-photo**	**TS-photo**	**Biradical**	**Biradical**	**Add**	**TS-dark**
electronic state	S_0	S_1	T_1	T_1	T_1	T_1	S_0	S_0	S_0
CAS(2,2)	−1304.576423	−1304.398784	−1304.443019	−1304.467340	−1304.424206	−1304.515333	−1304.520331	−1304.565059	−1304.479388
	(1)[b] 0.981	(2) 0.996	(2) 1.000	(2) 1.000	(2) 1.000	(2) 1.000	(1) 0.820	(1) 0.992	(1) 0.916
	(3) −0.196						(3) −0.573	(3) −0.124	(3) −0.399
MCQDPT2	−1307.440091	−1307.319140	−1307.346847	−1307.360405	−1307.342207	−1307.402101	−1307.411409	−1307.460488	−1307.394552
MRCI−SD[c]	−1304.627336	−1304.424324	−1304.503981	−1304.525280	−1304.479042	−1304.575831	−1304.557026	−1304.565597	−1304.525402
	(1) 0.952	(2) 0.950	(2) 0.948	(2) 0.954	(2) 0.957	(2) 0.961	(1) 0.851	(1) 0.992	(1) 0.914
	(3) −0.174	(5) 0.120	(5) 0.065	(8) −0.059	(8) −0.055	(8) 0.055	(3) −0.573	(3) −0.124	(3) −0.322
	(10) −0.088	(6) 0.113		(6) 0.051			(10) −0.070		(10) −0.073
		(7) 0.070							
CAS(4,4)	−1304.591664	−1304.421838	−1304.463504	−1304.489505	−1304.432498	−1304.532676	−1304.534528		−1304.493832
	(1) 0.969	(2) 0.957	(2) 0.977	(2) 0.976	(2) 0.995	(2) 0.986	(1) 0.810		(1) 0.907
	(3) −0.193	(6) −0.183	(8) −0.154	(8) −0.158	(8) −0.078	(8) −0.118	(3) −0.566		(3) −0.392
	(10) −0.146	(7) −0.121	(5) 0.070	(4) 0.065		(4) −0.091	(10) −0.116		(10) −0.134
							(11) 0.081		(11) 0.058
MCQDPT2	−1307.444489	−1307.320818	−1307.349785	−1307.366718	−1307.343690	−1307.402157	−1307.414647		−1307.397714
MRCI−SD[d]	−1304.631149	−1304.428096	−1304.509025	−1304.531495	−1304.486881	−1304.588301	−1304.562081		−1304.531630
	(1) 0.950	(2) 0.943	(2) 0.945	(2) 0.950	(2) 0.953	(2) 0.954	(1) 0.853		(1) 0.913
	(3) −0.172	(6) −0.164	(8) −0.135	(8) −0.141	(8) −0.071	(8) −0.106	(3) −0.464		(3) −0.312
	(10) −0.126	(7) −0.108	(5) 0.077	(9) 0.063	(5) 0.059		(10) −0.101		(10) −0.116
		(5) −0.107							

[a] The geometries were optimized by the CASSCF(2,2) method. [b] The CSFs specified by the occupancy numbers of the MOs within the (4,4) active space: (1) 2200, (2) 2110, (3) 2020, (4) 2101, (5) 1210, (6) 1111, (7) 1111, (8) 0112, (9) 0211, (10) 0202, and (11) 0022. [c] MOs obtained from the CASSCF(2,2) calculations were used. [d] MOs obtained from the CASSCF(4,4) calculations were used.

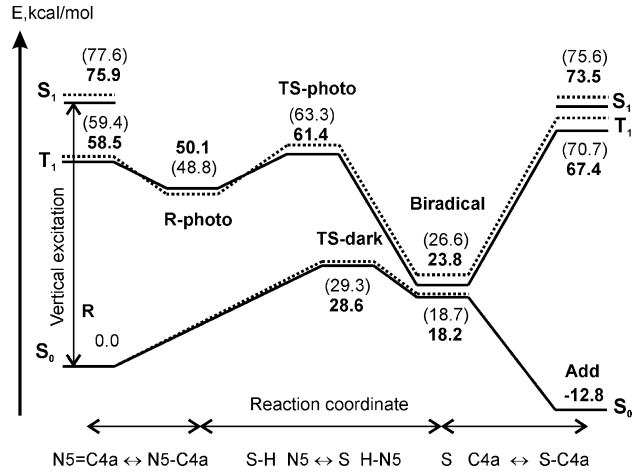

Figure 2. Energy diagram of the photocycle reactions between lumiflavin and thiomethanol derived from the single-point MCQDPT2/CASSCF(2,2) (solid line, bold numbers) and MCQDPT2/CASSCF(4,4) (dashed line, numbers in parentheses) calculations. The geometries of the model complexes were optimized by the CASSCF(2,2) method.

active space to (4,4) results in lowering the absolute energies of the electronic states without any significant changes of the relative energies (see also Figure 2) and the CI coefficients. Thus, for all considered geometries, the minimum active space (2,2) is sufficient for the description of the dynamic correlation.

The data from Table 1 is illustrated in Figure S1 in the Supporting Information. The diagrams show how the energies of the electronic states change when different electron correlation methods are employed. Accounting for dynamic correlation decreases the energies of the transition states **TS-photo** and **TS-dark** more than those of the reactant and product structures (Figure S1-B, Supporting Information). Therefore, the MCQDPT2 correction is significant for estimating the energy barrier heights for the photo- and dark reactions. Electrostatic charge distributions in the model complexes calculated by the CASSCF methods are presented in Table 2. As it is indicated for the **R** structure, virtually the same results were obtained with the (2,2) and (4,4) active space.

The unrestrained geometry optimization of the lumiflavin−thiomethanol complex results in an equilibrium structure where thiomethanol is located aside the isoalloxazine ring forming a hydrogen bond with the O4 atom (Figure S2 in the Supporting Information). There is no local minimum corresponding to a complex where thiomethanol occupies a position above the isoalloxazine ring. To obtain structure **R**, the geometry optimization in internal coordinates was carried out until the thiomethanol molecule started to move to the side of the isoalloxazine ring. In the resulting structure, the geometries of the thiomethanol and lumiflavin molecules are identical to those in the equilibrium structure. The S−C4a distance of 4.52 Å is similar to that of one of the Cys isomers in LOV1 (4.4 Å)[13] and a little longer than that in LOV2 (4.2 Å).[23]

In Figure 2, the energy profiles of the photocycle reactions derived from the MCQDPT2/CASSCF(2,2) and (4,4) calculations are superimposed. The relative energies of the model complexes (with respect to the energy of **R** in S_0) evaluated by these two methods agree within 0.5−3.3 kcal/mol. Unless otherwise stated, we will refer to the MCQDPT2/CASSCF(2,2) energy estimates (bold-type numbers in Figure 2). Vertical excitation to the S_1 state increases the energy of **R** to 75.9 kcal/mol. The vertical energy of the first triplet state T_1 is 58.5 kcal/mol. To obtain the structure of the triplet species, the geometry of complex **R** was further optimized in the T_1 state with the S−C4a distance fixed at 4.5 Å. The resulting structure **R-photo** is a complex between triplet lumiflavin and thiomethanol with a relative energy of 50.1 kcal/mol. Structural relaxation of the triplet lumiflavin involves an elongation of the N5−C4a bond from 1.27 to 1.38 Å and a shortening of the N5−C5 bond from 1.37 to 1.29 Å. In the triplet state, the H transfer between S−H and N5 has a 11.3 kcal/mol energy barrier [14.5 kcal/mol according to MCQDPT2/CASSCF(4,4)]. The barrier corresponds to the geometry **TS-photo** with S−H and H−N5 distances of 1.49 and 1.35 Å, respectively. Proton transfer coupled with electron transfer yields a biradical intermediate. Structure **Biradical** in Figure 1 was optimized with the S−C4a distance fixed at 3.40 Å, which was similar to the distance in **TS-photo**. Unrestrained geometry optimization resulted in a structure with the SCH_3 fragment aside of the

Table 2. Charge Distribution and Dipole Moments

method	CAS(2,2)	CAS(4,4)				CAS(2,2)	
structure	**R**	**R**	**R-photo**	**TS-photo**	**Biradical**	**Add**	**TS-dark**
electronic state	S_0	S_0	T_1	T_1	T_1	S_0	S_0
				Löwdin Atomic Charges (au)			
C5a	−0.023	−0.022	+0.132	+0.082	+0.048	+0.055	+0.006
N5	−0.050	−0.051	−0.233	−0.275	−0.214	−0.327	−0.204
C4a	−0.010	−0.009	+0.027	+0.042	−0.026	−0.052	−0.005
S	−0.067	−0.067	−0.071	−0.232	+0.026	+0.118	−0.053
H	+0.114	+0.114	+0.121	+0.232	+0.327	+0.310	+0.282
				Net Charges (au)			
$HSCH_3$	−0.003	−0.003	−0.005	−0.093			
SCH_3					+0.007	+0.095	−0.089
dipole moments (Debye)	10.0	10.0	10.8	12.2	6.6	5.5	9.6

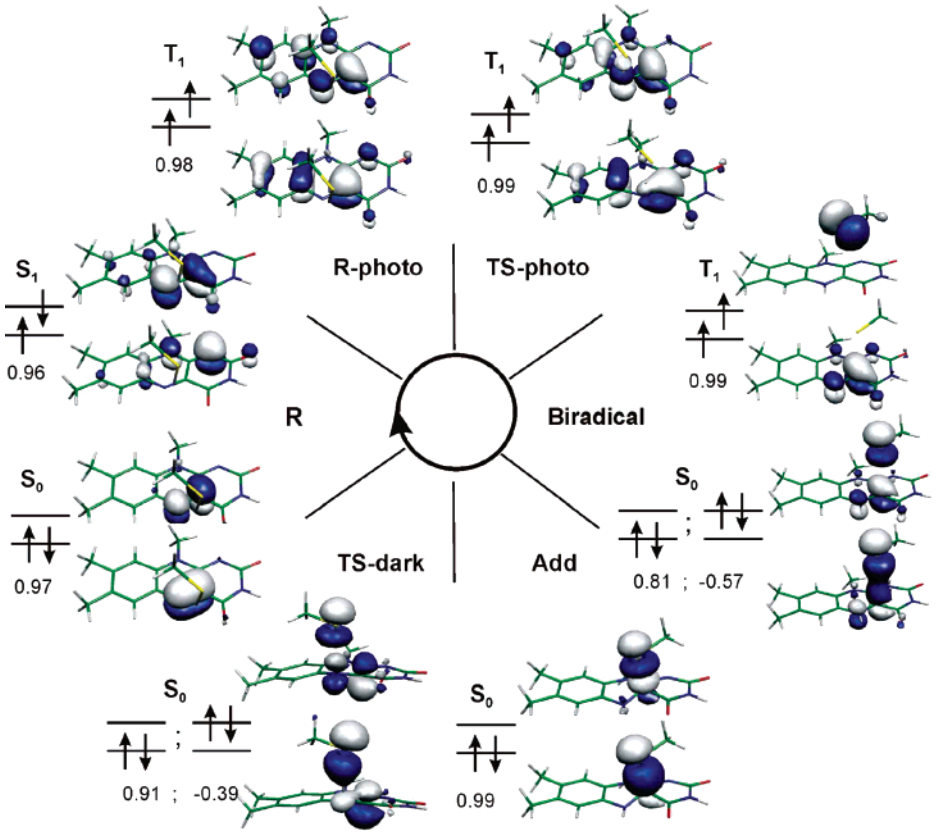

Figure 3. Electronic structure of the model complexes. Shown frontier molecular orbitals and the CI coefficients were optimized for a selected electronic state by the CASSCF(4,4) method. For the **Add** structure, the CASSCF(2,2) results are presented. The geometries of the model complexes were optimized by the CASSCF(2,2) method.

isoalloxazine ring (Figure S2 in the Supporting Information). **Biradical** contains two almost neutral radical fragments: HN5-semiquinone and thiomethyl radical SCH_3. The relative energies of **Biradical** are 23.8 and 18.2 kcal/mol in the T_1 and S_0 electronic states, respectively. In S_0, the energy of the complex decreases upon shortening of the S−C4a distance yielding the covalent adduct. A small energy difference between the two electronic states in the **Biradical** geometry indicates a possible crossing between the T_1 and S_0 states via a covalent bond formation between S and C4a. In the fully optimized structure **Add**, the equilibrium S−C4a bond distance is 1.92 Å. In the ground electronic state, the **Add** energy is 12.8 kcal/mol lower compared to that of **R.** A reverse of the photoreaction results in the dissociation of the covalent adduct via **TS-dark** with an energy barrier of 41.4 kcal/mol. The **TS-dark** structure is similar to **TS-photo** and has N−H and S−H distances of 1.10 and 1.78 Å, respectively, and a S−C4a distance of 3.38 Å.

The electronic structure of the model complexes occurring along the reaction coordinate is illustrated in Figure 3. In **R**, the electron excitation corresponds to a loss of the N5−C4a double bond. The S_1 and T_1 states of lumiflavin are of $\pi-\pi^*$ character. In T_1, the negative charge on N5 increases compared to the ground electronic state (Table 2). Interestingly, the positive charge on C5a occurs significantly higher than on C4a because of stabilization by the dimethylbenzene ring. In **R-photo**, unpaired electrons are rather delocalized. The product of the photoreaction **Biradical** has unpaired electrons localized on S, C4a, and N5. At the **Biradical** geometry, intersystem crossing takes place and the S−C4a σ bond forms in the ground state. Upon the **Add** dissociation, the N5═C4a double bond is partially restored in **TS-dark**.

Table 3. Energies of the Electronic Transitions (eV), Estimated by the State-Averaged MCQDPT2/CASSCF(2,2) and (4,4) Methods for the Singlet and Triplet Species, Respectively

molecular system	CASSCF (f_l^a)	MCQDPT2	exptl. LOV1[7], solution[35]
R (S_0-S_1)	4.53 (0.655)	2.86	2.77
R-photo (T_1-T_2)	1.99 (0.010)	1.64	1.73,1.88
Add (S_0-S_1)	5.13 (0.476)	3.37	3.18
lumiflavin[b] **(S_0-S_1)**	4.56 (0.670)	2.88	2.80
lumiflavin[c] **(T_1-T_2)**	2.20 (0.011)	1.49	1.95

[a] Oscillator strength. [b] S_0 RHF/6-31G(d) equilibrium geometry. [c] T_1 ROHF/6-31G(d) equilibrium geometry.

To further characterize the reactive complexes and to confirm that they can represent the LOV photospecies in terms of the electronic structure, the energies of the first electronic transitions S_0-S_1 and T_1-T_2 were evaluated by the state-averaged MCQDPT2/CASSCF calculations. The results are presented in Table 3. For comparison, the electronic transition energies in a free lumiflavin molecule in the ground and triplet electronic states were calculated in the RHF and ROHF/6-31G(d) equilibrium geometries, respectively. The S_0, S_1, T_1, and T_2 electronic states do not change within the reactant complexes with respect to a free lumiflavin molecule; therefore, the nature of the S_0-S_1 and T_1-T_2 transitions is the same, and the energies can be

compared. The CASSCF(2,2) method alone overestimates the transition energies, which can be improved by the MCQDPT2 correction.

All energy differences presented in Table 3 correspond to the $\pi-\pi^*$ electron excitations within the isoalloxazine fragment. The S_0-S_1 energy is virtually identical in the reactant species **R** and in the isolated lumiflavin molecule and somewhat larger compared to the experimental numbers. The calculated energy of the T_1-T_2 transition in both **R-photo** and free lumiflavin is significantly red-shifted when compared to the experimental results. Interestingly, despite that only π and π^* MOs of lumiflavin are involved in the transition, its energy is sensitive to the presence of the thiomethanol fragment, showing a blue shift in **R-photo** compared to lumiflavin. The T_1-T_2 transition has a small oscillator strength and, probably, is not visible in the experimental spectrum. The triplet species in LOV is characterized by a broad absorption peak with two maxima at 715 and 650−660 nm,[5,7] very similar to what is observed for the triplet flavins in a water solution.[36] In recent time-dependent DFT calculations,[37,38] the absorption of the triplet flavins around 700 nm was associated with the T_1-T_4 and T_1-T_5 transitions whose calculated energies were in satisfactory agreement with experimental results. Clearly, this subject requires more extensive analysis. Similarly to complex **R**, the predicted S_0-S_1 transition energy for the **Add** structure is overestimated with respect to the experimentally observed one. For the adduct complex, one should keep in mind that the transition energy calculated for the free compound is compared to the observations for the covalent adduct in the LOV protein. A larger difference between the calculated and observed transition energy of 0.2 eV obtained for **Add** compared to 0.1 eV obtained for **R** suggests that the absorption of the free covalent adduct may be slightly blue-shifted with respect to that of LOV. We could not confirm this suggestion by comparing experimental data because no data on a free flavin S−C4a adduct was available. However, it is known as a general trend that the low-energy absorption band of flavin C4a adducts around 380 nm is slightly shifted to the longer wavelength in the enzymes and also at a low temperature (77 K).[39]

The calculations of the electronic transitions in flavins are of great practical interest. Recently, absorption properties of different isoalloxazine molecules have been analyzed using DFT.[37,38,40] The S_0-S_1 transition in lumiflavin and riboflavin was predicted to be 3.05[37] and 3.07 eV,[38] respectively. Apparently, our MCQDPT2/CASSCF calculations with the minimal active space and a modest basis set are in better agreement with experimental results. Thus, multiconfigurational methods can be a very useful tool for spectroscopic applications in flavins.

The energy barrier structures **TS-photo** and **TS-dark** were determined using constrained optimization along the approximate reaction coordinate for hydrogen transfer between N5 and S. The reaction coordinate was specified by a decreasing N5−H or S−H distance for the photo- or dark reaction, respectively. Two dihedral angles determining the angle between S−N5 and the C5a−N5−C4a plane were fixed, ensuring the position of thiomethanol above the isoalloxazine ring. The other internal coordinates were optimized. In the obtained partly optimized geometry, the N5−H or S−H distance was further decreased and a new optimization step was performed to locate the following point of the energy scan. Such a stepwise procedure allows maximum structural relaxation of the molecular complex necessary to approach the intrinsic reaction coordinate. The calculated energy profiles are presented in Figures S3 and S4 in the Supporting Information. The drop of the energy of the complex is coupled with the major structural rearrangements such as breaking and formation of the N−H or S−H bonds when the system arrives at the product valley on the potential energy surface. In the photoreaction, the relaxation of the geometry after the hydrogen transfer to N5 includes the movement of the CH_3 group of thiomethanol from above the benzene ring to above the pyrimidine ring. The reverse movement was observed in the ground electronic state along the dark-reaction energy scan before the system reached the **TS-dark** geometry. A similar change in the conformation of the Cys side chain upon the covalent adduct formation is present in the X-ray crystal structures of the dark-adopted and light-illuminated LOV domains[13]. In the dark-reaction, the hydrogen transfer from N5−H to S follows the dissociation of the S−C4a covalent bond.

The highest-energy structures **TS-photo** and **TS-dark** are approximations for the saddle points. For both geometries, the calculated Hessians reveal two negative curvatures: one along the hydrogen-transfer intrinsic coordinate and the other for the rotation of the thiomethanol fragment. The corresponding imaginary frequencies (in cm^{-1}) are 835*i* (N5−H stretching) and 62*i* (SCH_3 rotation) in **TS-photo** and 1572*i* (S−H stretching) and 41*i* (SCH_3 rotation) in **TS-dark**. A saddle-point search starting from the **TS-photo** and **TS-dark** geometries was complicated by the movement of the thiol fragment away from its position above the isoalloxazine ring, yielding either the reactant or biradical equilibrium structure (Figure S2, Supporting Information). Nevertheless, we expect **TS-photo** and **TS-dark** to lie in the vicinity of the corresponding saddle points. Indeed, the **TS-photo** structure is similar to the saddle point located and confirmed by the vibrational analysis in the ROHF/6-31(2d,2p) QM/MM study[25] whose energy is 30.2 kcal/mol above the triplet state reactant. The lower activation energy in our model results from accounting for dynamic electron correlation. **TS-dark** is an analogue of **TS-photo** in the ground electronic state corresponding to the same chemical reaction—an addition of a thiol group to the N5═C4a double bond of an isoalloxazine. The energy barrier in the triplet state is significantly smaller than in the ground electronic state. The activation energies obtained for the photo- and dark reactions might be overestimated. Accounting for the vibrational energy typically decreases the energy barriers by several kilocalories per mole. In photoreactions, the population of the higher vibrational levels is common, which also decreases energy barriers and facilitates conversions. Both the photo- and dark reactions are single-step chemical transformations proceeding without intermediates.

The product of the photoreaction **Biradical** is unstable because of intersystem crossing. To characterize the crossing

geometry, we performed state-averaged CASSCF(4,3) calculations for the S_0 and T_1 electronic states (Figure S5 in the Supporting Information). The active space consisting of four electrons in three MOs was found (on the basis of the MRCI analysis for the state-averaged CASSCF wave function) to be sufficient to describe these electronic states simultaneously. In the **Biradical** geometry with a S−C4a distance of 3.40 Å, the S_0-T_1 energy difference calculated by the MCQDPT2/CASSCF(4,3) is 4.6 kcal/mol, which is in good agreement with the single-state estimates indicated in Figure 2. If the S−C4a distance increases, the S_0-T_1 energy difference becomes smaller. In a **Biradical**-like structure with a S−C4a distance of 4.5 Å, the MCQDPT2/CASSCF(4,3) S_0-T_1 energy difference is 1.4 kcal/mol. This structure lies in the vicinity of the S_0/T_1 crossing. A triplet intermediate similar to **Biradical** with an 18 kcal/mol energy barrier for the intersystem crossing was identified in LOV in the QM/MM model.[25] The predicted high stability of the biradical state is an artifact of the Hartree−Fock method used to compare the energies of the S_0 and T_1 electronic states. Our analysis shows (Table 1 and Figure 3) that the T_1 electronic state can be described by a single-determinant wave function, while the wave function of the S_0 electronic state should contain at least two determinants with occupied bonding π and antibonding π^* MOs. The S_0 energy of **Biradical** calculated with the two-configurational self-consistent field wave function is 41.3 kcal/mol lower than the Hartree−Fock energy. The decay of the triplet state biradical occurs via S−C4a covalent bond formation. It is very likely that, in different LOV domains, the S_0-T_1 energy difference for the crossing geometry can vary, resulting in different kinetics of the triplet state decay.

Structure **Add** aligns with the corresponding crystal structure (PDB: 1N9O)[13] with a root-mean-square deviation of 0.078 Å. According to the single-point MCQDPT2 calculations, the reaction energy of the addition of thiomethanol to the N5═C4a double bond of lumiflavin is −12.8 kcal/mol. The CASSCF method favors the reactant structure over the adduct by 7 kcal/mol, revealing a considerable contribution of the dynamic electron correlation to the adduct stability. To check the effect of the dynamic electron correlation, the geometries of the reactant and product complexes were optimized by the MP2/6-31G(d) method, which gave the reaction energy of −11.8 kcal/mol consistent with the single-point MCQDPT2 calculations. Interestingly, the S−C4a MP2 equilibrium distance is 1.87 Å, somewhat shorter than the CASSCF(2,2) equilibrium distance of 1.92 Å. The latter probably reflexes the tendency of the CASSCF-(2,2) to underestimate the product stability. The HF/6-31G-(d) equilibrium distance is 1.87 Å, in agreement with the MP2 optimization as well as the QM/MM optimization in LOV.[25] Despite the same equilibrium S−C4a distance, the HF method predicts a reaction energy of 1.3 and 8.7 kcal/mol[25] for the free compound and the LOV domain, respectively. Apparently, the stability of the covalent adduct is a property of a free compound. Therefore, we suggest that the protein matrix destabilizes the covalent adduct, which dissociates, however, with a high energy barrier.[41,42] To estimate the activation energy of the LOV dark-reaction using our model, the energy of **TS-dark** should be compared to the energy of **R** rather than the energy of **Add**. The relative energy of **TS-dark** gives an upper limit for the activation energy of the dark reaction. The decrease of the energy barrier depends on how much the S−C4a covalent adduct is destabilized in the protein and can be different in LOV1 and LOV2 domains.

Blue-light illumination of the LOV at $T = 77$ K yields a photoadduct absorbing at around 395 and 405 nm for LOV1 and LOV2, respectively.[16] This species, which is red-shifted compared to the room-temperature photoproduct absorbing at 390 nm, has been suggested to be a zwitterionic covalent adduct (Scheme 1B). The proposed mechanism of the photoreaction implied electron transfer from the thiol to FMN followed by recombination of the electron pair and a bond formation without proton transfer. We tested this hypothesis using our molecular model. Clearly, electron transfer from the thiol to the flavin does not take place upon excitation because complex **R-photo** consists of two uncharged fragments: the triplet lumiflavin and thiomethanol (Table 2). To form the zwitterion, electron transfer from the thiol to lumiflavin must be coupled with a shortening of the S−C4a distance. We calculated the energies of a series of lumiflavin−thiomethanol complexes with gradually decreasing S−C4a distances and with all other internal coordinates optimized in the triplet electronic state (Figure S6 in the Supporting Information). When the S−C4a distance was shortened to 2.4 Å, we observed a break of the C−S bond in thiomethanol, resulting in a release of the CH_3 radical. The lumiflavin−thiomethanol complex with a S−C4a distance of 2.6 Å is 12.7 kcal/mol above **R-photo** in the triplet state. The calculated positive net charge on $SHCH_3$ of +0.034 au is inconsistent with the suggestion that thiomethanol is an electron donor. We were not able to locate a minimum energy structure corresponding to the zwitterionic species in the ground electronic state. Thus, our results do not support the hypothesis that there is a pathway resulting in a zwitterionic S−C4a complex in the T_1 electronic state. Most likely, the cysteine does not reduce the triplet flavin unless it is deprotonated and electron-transfer coupled with proton transfer takes place in LOV. The specific location of the proton accepted by FMN within the S−H group situated above the FMN ring explains why the rate of the photoreaction is not pH-dependent, whereas it decreases in D_2O compared to that in a H_2O solution.[8,41,42]

Although our model does not account for the protein matrix, it allows suggestions concerning the role of the protein in the primary photoreaction of LOV. The positioning of the thiol above the isoalloxazine ring, which is arranged by the protein, is crucial for the chemistry because it ensures the interaction of the p atomic orbital centered on the sulfur atom with the π^* MO of the flavin, resulting in the S−C4a bond. The photoreaction in the free complex is unlikely to occur because the position of the thiol above the isoalloxazine ring is not stabilized by any intermolecular interaction. A **Biradical**-like geometry necessary for the efficient intersystem crossing is ensured by the protein. We suggest that the S−C4a covalent adduct spontaneously decays because the reactant state of the cofactor is favored by specific cofactor−

protein interactions including the change of the Cys conformation upon covalent binding as well as hydrogen bonds with the protein. One can notice that the hydrogen bonds between the FMN cofactor and the protein have shorter distances in the dark-adopted crystal structure model (PDB 1n9l) with respect to the distances in the covalent adduct model (PDB 1n9o) assuming that the LOV protein may work as a spring to facilitate the dissociation of the S−C4a adduct. Interestingly, the above prediction excludes acid−base catalysis of the dark reaction by the protein. This agrees with the crystal structures of LOV, where no potentially catalytic residues are present in the vicinity of the isoalloxazine chromophore.[13,22,23] Movement of the sulfur atom away from C4a to pick up the proton is possibly coupled with the transition between the two conformations of the reactive cysteine observed in the LOV1 crystal structure.[13]

To conclude, the mechanism of the primary photocycle reactions in LOV, which is rooted in the chemical properties of FMN and Cys and a specific geometry of the reagents arranged by the protein, can be accurately analyzed on a model system using MCQDPT2/CASSCF quantum-chemical calculations. In particular, the obtained electronic transition energies are in good agreement with the experimental data of LOV. The electronic structure of the reactants, adduct, and the triplet state species is adequately described by single-determinant wave functions. One should account for the dynamic electron correlation to estimate the energy barrier of the H transfer and the reaction energy. A multiconfigurational representation of the wave function is important to describe the formation and dissociation of the C−S4a bond and to estimate the stability of the biradical intermediate. Both the light-induced and dark reactions proceed with a concerted mechanism with a single energy barrier corresponding to a hydrogen transfer. The protein plays a minor role in stimulating the chemical reactivity of the FMN cofactor in LOV, being, however, crucial for the specific positioning of the cysteine above the isoalloxazine ring as well as the destabilization of the photoproduct and determination of the conformational space of the dark reaction.

Acknowledgment. We are very grateful to Roger Goody for his generous hospitality and support and acknowledge the DFG (FOR526) for funding.

Supporting Information Available: Cartesian coordinates of the model complexes, the diagrams illustrating the data presented in Table 1, absolute energies calculated with the state-averaged energy functional, results of the energy scanning for the photo- and dark reactions, energy profile for the **Biradical** recombination. This material is available free of charge via the Internet at http://pubs.acs.org.

References

(1) Christie, J. M.; Reymond, P.; Powell, G. K.; Bernasconi, P.; Raibekas, A. A.; Liscum, E.; Briggs, W. R. *Science* **1998**, *282*, 1698−1701.

(2) Christie, J. M.; Salomon, M.; Nozue, K.; Wada, M.; Briggs, W. R. *Proc. Natl. Acad. Sci. U.S.A.* **1999**, *96*, 8779−8783.

(3) Christie, J. M.; Briggs, W. R. *J. Biol. Chem.* **2001**, *276*, 11457−11460.

(4) Taylor, B. L.; Zhulin, I. B. *Microbiol. Mol. Biol. Rev.* **1999**, *63*, 479−506.

(5) Salomon, M.; Christie, J. M.; Knieb, E.; Lempert, U.; Briggs, W. R. *Biochemistry* **2000**, *39*, 9401−9410.

(6) Salomon, M.; Eisenreich, W.; Durr, H.; Schleicher, E.; Knieb, E.; Massey, V.; Rudiger, W.; Muller, F.; Bacher, A.; Richter, G. *Proc. Natl. Acad. Sci. U.S.A.* **2001**, *98*, 12357−12361.

(7) Kottke, T.; Heberle, J.; Hehn, D.; Dick, B.; Hegemann, P. *Biophys. J.* **2003**, *84*, 1192−1201.

(8) Swartz, T. E.; Corchnoy, S. B.; Christie, J. M.; Lewis, J. W.; Szundi, I.; Briggs, W. R.; Bogomolni, R. A. *J. Biol. Chem.* **2001**, *276*, 36493−36500.

(9) Song, P. S. *Photochem. Photobiol.* **1968**, *7*, 311.

(10) Miura, R. *Chem. Rec.* **2001**, *1*, 183−194.

(11) Drossler, P.; Holzer, W.; Penzkofer, A.; Hegemann, P. *Chem. Phys.* **2002**, *282*, 429−439.

(12) Kowalczyk, R. M.; Schleicher, E.; Bittl, R.; Weber, S. *J. Am. Chem. Soc.* **2004**, *126*, 11393−11399.

(13) Fedorov, R.; Schlichting, I.; Hartmann, E.; Domratcheva, T.; Fuhrmann, M.; Hegemann, P. *Biophys. J.* **2003**, *84*, 2474−2482.

(14) Kennis, J. T.; Crosson, S.; Gauden, M.; van Stokkum, I. H.; Moffat, K.; van Grondelle, R. *Biochemistry* **2003**, *42*, 3385−3392.

(15) Ataka, K.; Hegemann, P.; Heberle, J. *Biophys. J.* **2003**, *84*, 466−474.

(16) Schleicher, E.; Kowalczyk, R. M.; Kay, C. W. M.; Hegemann, P.; Bacher, A.; Fischer, M.; Bittl, R.; Richter, G.; Weber, S. *J. Am. Chem. Soc.* **2004**, *126*, 11067−11076.

(17) Kay, C. W.; Schleicher, E.; Kuppig, A.; Hofner, H.; Rudiger, W.; Schleicher, M.; Fischer, M.; Bacher, A.; Weber, S.; Richter, G. *J. Biol. Chem.* **2003**, *278*, 10973−10982.

(18) Heelis, P. F.; Parsons, B. J.; Phillips, G. O.; McKellar, J. F. *Photochem. Photobiol.* **1979**, *30*, 343−347.

(19) Bittl, R.; Kay, C. W.; Weber, S.; Hegemann, P. *Biochemistry* **2003**, *42*, 8506−8512.

(20) Kottke, T.; Dick, B.; Fedorov, R.; Schlichting, I.; Deutzmann, R.; Hegemann, P. *Biochemistry* **2003**, *42*, 9854−9862.

(21) Richter, G.; Weber, S.; Romisch, W.; Bacher, A.; Fischer, M.; Eisenreich, W. *J. Am. Chem. Soc.* **2005**, *127*, 17245−17252.

(22) Crosson, S.; Moffat, K. *Proc. Natl. Acad. Sci. U.S.A.* **2001**, *98*, 2995−3000.

(23) Crosson, S.; Moffat, K. *Plant Cell* **2002**, *14*, 1067−1075.

(24) Neiss, C.; Saalfrank, P. *Photochem. Photobiol.* **2003**, *77*, 101−109.

(25) Dittrich, M.; Freddolino, P. L.; Schulten, K. *J. Phys. Chem. B* **2005**, *109*, 13006−13013.

(26) Losi, A.; Kottke, T.; Hegemann, P. *Biophys. J.* **2004**, *86*, 1051−1060.

(27) Pulay, P.; Fogarasi, G. *J. Chem. Phys.* **1992**, *96*, 2856−2860.

(28) Schmidt, M. W.; Gordon, M. S. *Annu. Rev. Phys. Chem.* **1998**, *49*, 233−266.

(29) Nakano, H. *J. Chem. Phys.* **1993**, *99*, 7983−7992.

(30) Lowdin, P. O. *Phys. Rev.* **1955**, *97*, 1474−1489.

(31) Mulliken, R. S. *J. Chem. Phys.* **1955**, *23*, 1833−1840.

(32) Granovsky, A. A. PC Gamess. http://classic.chem.msu.su/gran/gamess/index.html (accessed Mar 2004).

(33) Schmidt, M. W.; Baldridge, K. K.; Boatz, J. A.; Elbert, S. T.; Gordon, M. S.; Jensen, J. H.; Koseki, S.; Matsunaga, N.; Nguyen, K. A.; Su, S. J.; Windus, T. L.; Dupuis, M.; Montgomery, J. A. *J. Comput. Chem.* **1993**, *14*, 1347−1363.

(34) Flükiger, H. P.; Lüthi, S.; Portmann, J. *MOLEKEL 4.2*; Weber and Swiss Center for Scientific Computing: Manno, Switzerland, 2003.

(35) Sikorska, E.; Khmelinskii, I. V.; Koput, J.; Sikorski, M. *THEOCHEM* **2004**, *676*, 155−160.

(36) Sakai, M.; Takahashi, H. *J. Mol. Struct.* **1996**, *379*, 9−18.

(37) Neiss, C.; Saalfrank, P.; Parac, M.; Grimme, S. *J. Phys. Chem. A* **2003**, *107*, 140−147.

(38) Sikorska, E.; Khmelinskii, I.; Komasa, A.; Koput, J.; Ferreira, L. F. V.; Herance, J. R.; Bourdelande, J. L.; Williams, S. L.; Worrall, D. R.; Insinska-Rak, M.; Sikorski, M. *Chem. Phys.* **2005**, *314*, 239−247.

(39) Ghisla, S.; Massey, V.; Lhoste, J. M.; Mayhew, S. G. *Biochemistry* **1974**, *13*, 589−597.

(40) Insinska-Rak, M.; Sikorska, E.; Herance, J. R.; Bourdelande, J. L.; Khmelinskii, I. V.; Kubicki, M.; Prukala, W.; Machado, I. F.; Komasa, A.; Ferreira, L. F. V.; Sikorski, M. *Photochem. Photobiol. Sci.* **2005**, *4*, 463−468.

(41) Corchnoy, S. B.; Swartz, T. E.; Lewis, J. W.; Szundi, I.; Briggs, W. R.; Bogomolni, R. A. *J. Biol. Chem.* **2003**, *278*, 724−731.

(42) Guo, H.; Kottke, T.; Hegemann, P.; Dick, B. *Biophys. J.* **2005**, *89*, 402−412.

CT0600114